© 2017. Published by The Company of Biologists Ltd | Journal of Experimental Biology (2017) 220, 227-236 doi:10.1242/jeb.146449

RESEARCH ARTICLE

Developmental changes in head movement kinematics during swimming in *Xenopus laevis* tadpoles

Sara Hänzi[1,2,*] and Hans Straka[1]

ABSTRACT

During the post-embryonic developmental growth of animals, a number of physiological parameters such as locomotor performance, dynamics and behavioural repertoire are adjusted to match the requirements determined by changes in body size, proportions and shape. Moreover, changes in movement parameters also cause changes in the dynamics of self-generated sensory stimuli, to which motion-detecting sensory systems have to adapt. Here, we examined head movements and swimming kinematics of *Xenopus laevis* tadpoles with a body length of 10–45 mm (developmental stage 46–54) and compared these parameters with fictive swimming, recorded as ventral root activity in semi-intact *in vitro* preparations. Head movement kinematics was extracted from high-speed video recordings of freely swimming tadpoles. Analysis of these locomotor episodes indicated that the swimming frequency decreased with development, along with the angular velocity and acceleration of the head, which represent self-generated vestibular stimuli. In contrast, neither head oscillation amplitude nor forward velocity changed with development despite the ∼3-fold increase in body size. The comparison between free and fictive locomotor dynamics revealed very similar swimming frequencies for similarly sized animals, including a comparable developmental decrease of the swimming frequency. Body morphology and the motor output rhythm of the spinal central pattern generator therefore develop concurrently. This study thus describes development-specific naturalistic head motion profiles, which form the basis for more natural stimuli in future studies probing the vestibular system.

KEY WORDS: Locomotion, Tadpole, Body morphology, Central pattern generator, Vestibular system

INTRODUCTION

During development, when animals grow in size with species-specific modifications of body size, form and proportion, the dynamics of the locomotor mechanisms and the sensory feedback have to concurrently adapt to maintain or even improve motor performance. Specific modifications of propulsive structural elements and motion detection systems are required to ensure both optimal motor output and maintenance of an adequate sensitivity and working range of the sensory organs, as self-motion activates responses of various sensory modalities such as the visual and vestibular systems (Carriot et al., 2014; Wark et al., 2007). Thus, quantification of locomotor performance allows the extraction of species-specific kinematic parameters of the propulsive mechanisms as well as inference of the stimulus statistics of self-generated sensory inputs. Moreover, comparing locomotor characteristics during development – in particular, in fish and amphibians, which develop through a series of fast-growing larval stages with changes in body proportions and form – allows alterations in body size and sensory capacity to be related to concurrent changes in locomotor dynamics.

Many studies have added to the current knowledge of the development of the motor program underlying free swimming in *Xenopus laevis* tadpoles (see Roberts et al., 2010), zebrafish (Brustein et al., 2003; Saint-Amant and Drapeau, 1998) and angelfish (Yoshida et al., 1996), on both a behavioural and a neural circuit level. However, little is known about how the kinematic parameters of swimming change during larval development, when the relative body proportions change and the size of the animals and their appendages increase considerably. While a previous anecdotal report described some aspects of locomotion in a very small number of older *Xenopus laevis* tadpoles at an unspecified developmental stage (Hoff and Wassersug, 1986), a systematic evaluation of head/body movements and quantification of alterations in swimming kinematics during larval development is lacking. A major advantage of using *X. laevis* for such an analysis is the solid knowledge about the embryonic and early larval development of the spinal motor circuitry (Harland and Grainger, 2011; Roberts et al., 2010; Wallingford et al., 2010). In addition, the ability to perform *in vitro* experiments on isolated semi-intact preparations (Straka and Simmers, 2012; Straka et al., 2016) allowed the consequences of locomotor activity on the processing of head/body motion-related sensory signals to be studied (Chagnaud et al., 2015; Lambert et al., 2012a). A description of developmental changes in locomotor dynamics during larval life will facilitate the understanding of how swimming kinematics and the capacity of vestibular sense organs for motion detection might influence each other.

Here, we used *X. laevis* tadpoles with a length of 10–45 mm (developmental stages 46–56 according to Nieuwkoop and Faber, 1956) to reveal how swimming kinematics change during the period when the animals experience their largest growth in body size. The movements of the larvae in the horizontal plane during episodes of free swimming were captured with a video camera from above to quantify locomotor parameters such as swimming frequency and forward velocity, as well as angular velocity and acceleration, from the tightly coupled head/tail movements that are relevant as stimuli for the activation of vestibular organs (Chagnaud et al., 2012). The obtained natural stimulus statistics of self-generated vestibular signals allowed estimation of the size-related impact of self-motion on the activation of responses in hair cells of the semicircular canal organs. Comparison of the characteristics of locomotor performance during free and fictive swimming – the latter obtained from electrophysiological recordings in stationary *in vitro* preparations – addressed the question of whether any potential changes in locomotor parameters during development required online sensory feedback

[1]Department of Biology II, Ludwig-Maximilians-University Munich, Großhaderner Strasse 2, Planegg 82152, Germany. [2]Graduate School of Systemic Neurosciences, Ludwig-Maximilians-University Munich, Großhaderner Strasse 2, Planegg 82152, Germany.

*Author for correspondence (haenzi@bio.lmu.de)

Received 19 July 2016; Accepted 23 October 2016

Journal of Experimental Biology (2017) 220, 227-236 doi:10.1242/jeb.146449

(in which case the change would be a short-term adaptation according to the terminology of Pearson, 2000), or whether these changes persisted in the absence of immediate sensory feedback, in which case they would be long-term adaptations.

MATERIALS AND METHODS

Animals

Experiments were performed on tadpoles of the African clawed toad, *Xenopus laevis* Daudin 1802, of either sex at developmental stages 46–56 (Nieuwkoop and Faber, 1956) with a size of 10–45 mm. Animals at different developmental stages were identified according to stage-specific morphological features in freely moving animals in a Petri dish under a dissection microscope. Tadpoles were obtained from the in-house breeding facility at the Biocentre of the Ludwig-Maximilians-University Munich, where all animals were kept in aerated tanks at 17°C on a 12 h:12 h light:dark cycle. All behavioural observations as well as electrophysiological experiments on isolated, semi-intact *in vitro* preparations complied with the 'Principles of animal care', publication no. 86-23, revised 1985, of the National Institutes of Health. Permission for experiments was granted by the Regierung von Oberbayern (55.2-1-54-2532.3-59-12).

Video recordings of locomotor activity

The locomotor performance of tadpoles (N=25 animals) was evaluated by video recordings of the swimming activity in a 7×7 cm tank with a water depth of 1–1.2 cm. The water was maintained at a constant temperature of 17°C by placing the tank into a larger (20×20 cm) container, filled with approximately 1 litre of water, that allowed regulation of the temperature. Videos were acquired with a Point Grey Grasshopper3 camera (GS3-U3-23S6M-C, Point Grey, Richmond, Canada) using Fly Capture software (version 2.8.3.1). The spatial resolution was 960×960 pixels, and the temporal resolution was ∼200 frames s^{-1}; the images were saved as series of separate tiff files. The time stamp of each frame was read out individually from the camera's internal cycle running at 8 kHz. Animals in the tank were filmed from above with lighting provided from below (ZLED CLS6000, Zett Optics GmbH, Braunschweig, Germany). Recordings were started and terminated manually to maximise recording episodes of swimming events when the animal was not touching one of the four vertical walls. While on some occasions the animals spontaneously swam through the centre of the tank, most of the time the tadpoles followed a trajectory along the vertical walls. In order to increase the number of unimpaired swimming episodes through the centre of the tank, animals were gently touched to redirect the swimming trajectory.

Data analysis

The tiff files from the videos were opened in Fiji (http://fiji.sc/Fiji) and visually inspected for wall touch by the tadpoles. Episodes without wall touch were further analysed by thresholding the images such that the eyes formed distinct black shapes. These objects were tracked using the MTrack2 plugin (http://valelab.ucsf.edu/~nstuurman/ijplugins/MTrack2.html; Fig. 1A) and the tracking results were saved as text files. The text files were then imported into Matlab (Mathworks, Natick, MA, USA) and analysed with custom-written scripts that calculated the angle of the line formed by the centroids of the eyes relative to an external but arbitrary reference. This procedure allowed determination of the head angle in space over time during a swimming episode (Fig. 1A,C). The timing was extracted from the time stamp assigned to each frame by the camera from its internal 8 kHz cycler (see above). The head angle trace was smoothed using a third-order polynomial Savitzky–Golay filter based on seven consecutive time points (Fig. 1C). The smoothed trace was then used to calculate the angular velocity by dividing the difference in head angle between two frames by the time difference. This procedure was repeated to calculate the angular acceleration. To calculate forward velocity, the distance covered between subsequent frames by the interocular midpoint was determined and divided by the time difference between the two frames. The Reynolds number (Re) was calculated as $Re=U\times L/\nu$, where U is forward velocity in mm s^{-1}, L is total length of the animal and ν is kinematic viscosity of water at 17°C (1.0811 mm^2 s^{-1}; see http://www.viscopedia.com/viscosity-tables/substances/water/). The frequency and amplitude of the head oscillations during each swimming episode were calculated based on the left–right alternating peaks of the head angle trace. The amplitude between the peak in one direction and the next peak in the other direction was determined as the half-cycle amplitude (i.e. one right–left or left–right movement of the head), and the corresponding duration was determined as the time required for half a swimming cycle period. From this half-period, we calculated the instantaneous head oscillation frequency, which directly corresponds to the tail-beat frequency, as the head and trunk are tightly coupled (Chagnaud et al., 2012), and will be referred to as swimming frequency throughout the study.

From over 400 swimming episodes without wall touch, selected episodes were further analysed based on the criterion of at least six consecutive head oscillations (i.e. half-cycles) with an amplitude between 4 and 90 deg, to exclude image jitter as well as very large turns such as escape-related C-starts. These selected episodes from the same animal were pooled, and the median and interquartile ranges for each animal are reported.

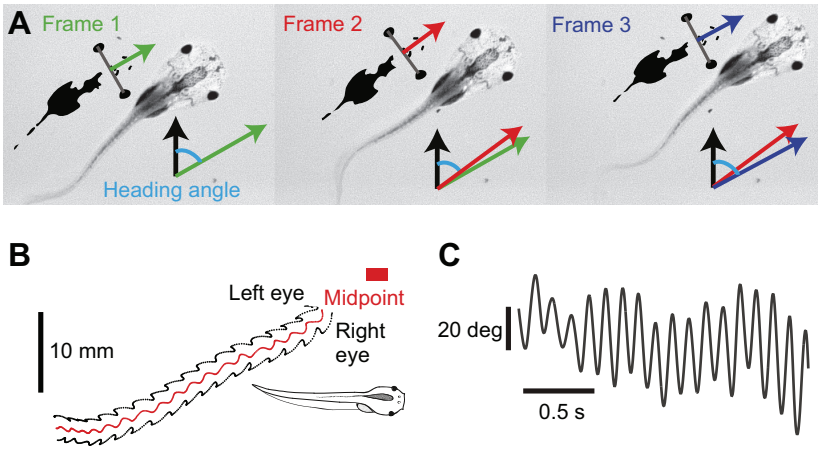

Fig. 1. Extraction of parameters of head movement kinematics. (A) Sequence of three video frames separated by ∼80 ms, depicting the dorsal view of a stage 50 tadpole during free swimming along with the thresholded black-and-white image of the animal as an inset. From the thresholded image, the position of the eyes was extracted, and the angle of the heading direction was calculated (coloured forward arrow). (B) Trajectories of the two eyes (black dots) and interocular midpoint (red), obtained from a video recording at 200 frames s^{-1} of a 2 s swim episode in a stage 48 tadpole. Tadpole scheme from Hänzi and Straka (2016a). (C) Head angles calculated from the trajectory in B, indicating very regular left–right head oscillations during swimming.

Journal of Experimental Biology (2017) 220, 227-236 doi:10.1242/jeb.146449

Anatomical measurements

To correlate the extent of morphological changes with the different developmental stages, the following parameters were extracted from the videos: distance between the eyes (interocular distance), total length of the animal, trunk length, and tail width at the level of the hindlimbs. The interocular distance was determined as the median of the distance between the two eyes in all frames of a particular animal. The remaining parameters were manually extracted using Fiji based on two frames each from two different video recordings of the same animal. The final value was then calculated as the mean of these four values.

Fictive swimming: electrophysiology

To compare the frequency of free swimming with fictive swimming – which excludes biomechanical properties of tail motion as well as the corresponding proprioceptive feedback – multi-unit ventral root spiking activity was recorded in stationary semi-intact *in vitro* preparations of larvae at different developmental stages. Some of the data that were included in the present study (13 out of 18 animals) were obtained in the framework of a previous study (Hänzi et al., 2015). Semi-intact preparations were obtained based on the procedure described previously (Hänzi et al., 2015). Briefly, tadpoles were anaesthetised using 0.05% 3-aminobenzoic acid ethyl ester (MS-222; Sigma-Aldrich, UK), decapitated and decerebrated in ice-cold Ringer solution (composition in mmol l^{-1}: NaCl, 75; KCl, 2; $CaCl_2$, 2; $MgCl_2$, 0.5; $NaHCO_3$, 25; glucose, 11; pH 7.4). The spinal cord was exposed approximately from segment 2 to segment 15, with the remaining part of the tail left intact. The ventral roots along the exposed spinal cord were cut, the trunk muscles removed, and the preparation was transferred into the recording chamber, where it was continuously superfused with freshly oxygenated Ringer solution at a rate of about 1–3 ml min^{-1} while the temperature was kept at 17±0.5°C. One or more ventral roots of spinal segments 8–15 were recorded using glass suction electrodes (pulled on a P-97 Brown/Flaming puller, Sutter Instruments, Novato, CA, USA) with the tip individually adjusted to the size of the nerve roots. Fictive swimming occurred either spontaneously or following gentle touch of the caudal part of the tail or the otic capsule. Signals were amplified (EXT 10-2F; npi electronics, Tamm, Germany), digitised at 10 kHz (CED 1401, Cambridge Electronic Design, Cambridge, UK), recorded using Spike2 (Cambridge Electronic Design) and stored for subsequent off-line analysis.

Episodes of fictive swimming, identified by rhythmic ventral root activity (Combes et al., 2004), were exported from Spike2 into Matlab; episodes of fictive struggle or potential escape responses, indicated by strong concurrent bilateral and single alternating bursting, were excluded from further analysis. The spike discharge was extracted using custom-written scripts based on code written by Daniel Wagenaar (http://www.its.caltech.edu/~daw/teach.html#matlab). Briefly, spikes were extracted using a threshold based on the noise level in the recording trace (5 times the root mean square) and bursts were defined as at least two spikes with maximal inter-spike intervals of 20–70 ms. The swimming frequency was then determined as the inverse of the inter-burst interval within one ventral root.

Statistics

Statistical analysis was carried out in Matlab using custom-written scripts. Distributions were tested for normality using the Shapiro–Wilk test; if significant, the appropriate non-parametric test was used. To test for changes across development, a regression of the total length of the animal to the median value per animal was calculated for each kinematic parameter. $P<0.05$ was considered significant.

RESULTS

Increase of body size during development

The post-embryonic, larval development in amphibians is generally characterised by a considerable increase in body size (Fig. 2A; also see Nieuwkoop and Faber, 1956). Determination of body and trunk length, interocular distance and tail width at the level of the emerging hindlimbs (Fig. 2B) revealed that these parameters increased steadily and correlated with developmental stage (N=35; Fig. 2C–F) previously used to describe the progressive steps of *X. laevis* ontogeny (Nieuwkoop and Faber, 1956). The size of the tadpoles (total body length) employed in the current study ranged between ∼10 mm for the youngest (stage 46) and ∼45 mm for the oldest animals (stage 56; Fig. 2C). This parameter reliably predicted the developmental stages of *Xenopus* tadpoles (Fig. 2C). This prediction was equally well achieved with the other measured parameters such as trunk length (Fig. 2D), interocular distance

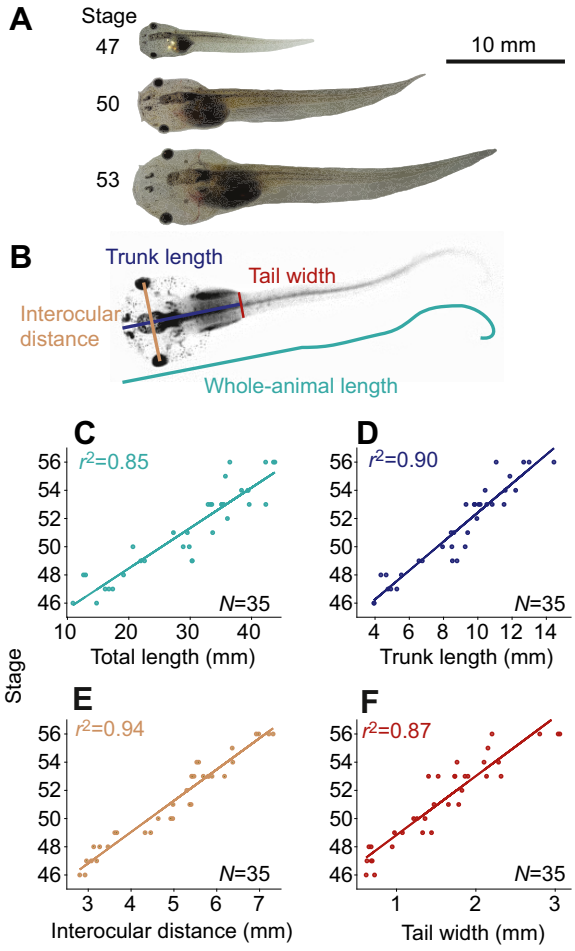

Fig. 2. Tadpole growth. (A) Images of *Xenopus* tadpoles on the same scale, with the developmental stage indicated (modified from Hänzi and Straka, 2016b). (B) Illustration of the anatomical parameters, extracted from a video frame of a stage 51 animal (see Materials and methods for details). (C–F) Developmental changes of the total length of the animal (C), trunk length (D), interocular distance (E) and tail width at the position where the hindlimbs emerge (F) in a total of 35 animals. Note the high r^2 values of linear regressions of all parameters with respect to developmental stage.

Journal of Experimental Biology (2017) 220, 227-236 doi:10.1242/jeb.146449

(Fig. 2E) and tail width (Fig. 2F). This was surprising, given the fact that developmental stages in *X. laevis* tadpoles were defined on the basis of multiple morphological features including the progression of limb growth and differentiation or the size and visibility of visceral organs (Nieuwkoop and Faber, 1956). Even though all extracted anatomical parameters were able to predict developmental advancement, we used total body length as linear regressor, thereby facilitating comparisons with other studies.

Kinematic parameters

Video tracking of tadpoles (Fig. 1A) was used to extract the position of both eyes and thereby to determine the trajectory of the animal during episodes of free swimming (Figs 1B, 3A). These data on eye position served to calculate the angle of the head over time relative to an external but arbitrary reference (Figs 1C, 3B). From the excursions of the head angle, the amplitude of the head oscillations was determined (Fig. 3D, indicated as amplitude), as well as the 'instantaneous' swimming frequency (Fig. 3C). Furthermore, angular acceleration and velocity were calculated from the head angle (Fig. 3E,F) using the time stamp of each frame as precise timing information. Finally, from the interocular midpoint (red in Fig. 3A) and the timing information, the animal's forward velocity was determined (Fig. 3G). The two examples of differently sized animals (stages 48 and 54) shown in Fig. 3 indicate that the swimming performance of smaller larvae differs considerably from that of larger animals in some of the kinematic parameters (trajectories on the left and right of Fig. 3A are shown on the same spatial scale; see also Movies 1 and 2). Notably, the head/tail oscillations during an example swimming episode of a young tadpole (13 mm, stage 48, green) generally occurred at higher frequencies (Fig. 3C) compared with those of an older animal (38 mm, stage 54, blue). Accordingly, swimming in the younger tadpole is characterised by higher angular velocity and acceleration (Fig. 3E,F). However, the maximal forward velocity was similar despite the differences in body size (Fig. 3G).

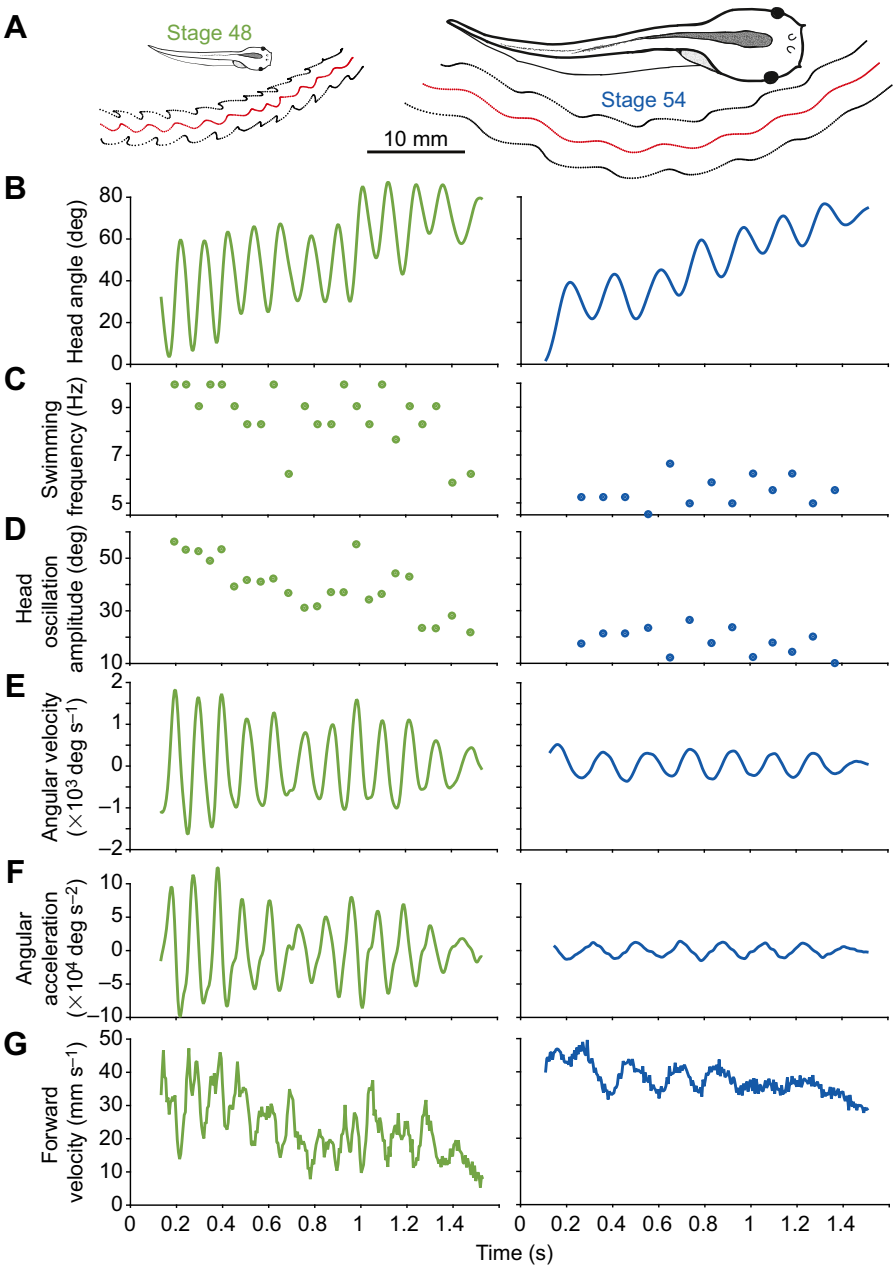

Fig. 3. Examples of swimming episodes of two differently sized larvae along with extracted kinematic parameters. (A) Swimming trajectories of a 13 mm-long stage 48 (left) and a 38 mm-long stage 54 (right) tadpole over a period of 1.4 s. Eye positions (black trajectories) and interocular midpoints (red trajectory) were obtained from video recordings at 200 frames s^{-1}. These sequences were obtained from Movies 1 and 2. The trajectories and animal drawings are shown on the same scale (drawings from Hänzi and Straka, 2016a). (B) Angle of the head over time extracted from the trajectories shown in A. (C,D) Swimming frequency (C) and amplitude (D) of head oscillations over time calculated from the head angle oscillations shown in B. (E,F) Angular velocity (E) and acceleration (F) of the head over time during the swimming episodes shown in A, calculated from smoothed head angle (B) and velocity (E) traces, respectively (see Materials and methods). (G) Forward velocity calculated from the distance covered by the interocular midpoint during the swimming episodes shown in A.

Journal of Experimental Biology

Journal of Experimental Biology (2017) 220, 227-236 doi:10.1242/jeb.146449

Consistency of kinematic parameters over repeated swimming episodes

Episodes of free swimming for quantitative analysis were selected based on two criteria: first, the animal did not touch a vertical wall and second, at least six consecutive half-cycles of swimming (i.e. left–right or right–left head movements) were within an amplitude range between 4 and 90 deg (see Materials and methods for details). The consistency of the kinematic parameters over multiple swimming episodes within the same animal was tested for those parameters that were extracted on the basis of each half-cycle. The frequency and amplitude distribution of the 15 swimming episodes of a 13 mm stage 48 tadpole are shown in Fig. 4A,C, with the different episodes plotted on the *y*-axis and the half-cycles within each episode represented as bars on the *x*-axis. The presence of mostly blue–green bars in the colour-coded representation (Fig. 4A) indicated that the swimming frequency within a given episode as well as between different episodes was relatively consistent. In contrast, the amplitude of the head oscillations varied considerably both within and between episodes, as implied by the widely different colours within and between episodes (Fig. 4C).

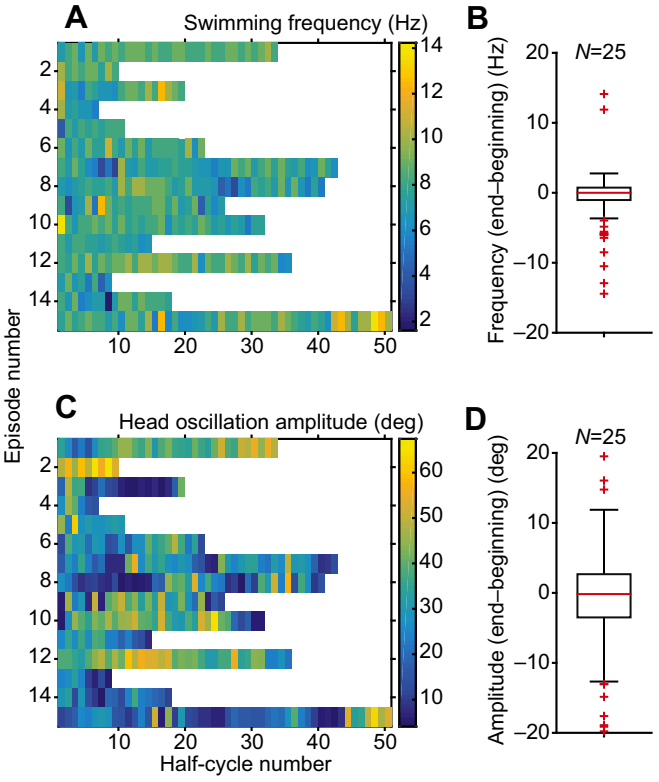

Fig. 4. Intra-animal variability of swimming frequency and head oscillation amplitude. (A,C) Colour-coded swimming frequency (A) and head oscillation amplitude (C) across 15 episodes (*y*-axis) in a 13 mm stage 48 tadpole, with the number of half-cycles indicated on the *x*-axis. The relatively uniform colour distribution in A indicates little intra- and inter-episodal variability of the swimming frequency, whereas the large variation of the colour in C shows a considerable intra- and inter-episodal variability of head oscillation amplitude in this typical animal. (B,D) Boxplot depicting the difference in the mean frequency (B) and the mean head oscillation amplitude (D) of the first and last two half-cycles of a given episode (221 episodes from *N*=25 animals). Note the spread of differences either side of zero in B and D, indicating that the distribution of differences between the beginning and end of the episode is not significantly different from zero (one-sample Wilcoxon signed-rank tests; the *y*-axis was cropped for both plots) and, thus, the frequency and amplitude of swimming were very similar at the beginning and end of each swimming episode.

As previous reports on swimming *X. laevis* hatchlings reported that the frequency of the head/tail oscillations decreased gradually over the course of a given swimming episode (Kahn et al., 1982; Sillar and Roberts, 1993; Sillar et al., 1991), the difference between the mean frequency of the first two and the last two half-cycles of each episode was calculated (Fig. 4B; 221 episodes in *N*=25 animals) and found not to be significantly different from zero (one-sample Wilcoxon signed-rank test, $P>0.05$). Similarly, the difference between the amplitude of the head oscillation at the beginning and the end of each swim episode was not statistically different from zero either (Fig. 4D; 221 episodes in *N*=25 animals, one-sample Wilcoxon signed-rank test, $P>0.05$).

Changes in kinematic parameters with development

To compare the kinematic parameters of swimming in animals with progressively larger total body length, all episodes for a given animal were pooled, and the median and interquartile ranges per animal (*N*=25) were plotted. The largest change was observed for the frequency of swimming, which decreased considerably with growth (Fig. 5A; regression of total length of the animal against its median swimming frequency: $r^2=0.77$, $P<0.0001$). In contrast, the amplitude of the head oscillations was relatively variable within each animal (see Fig. 4), and the median amplitude remained relatively constant across the differently sized animals (Fig. 5B; regression of total length against median amplitude, $P>0.05$). The median angular velocity and acceleration during swimming in the smallest animals were remarkably high: ∼150–600 deg s^{-1} and ∼5000–20,000 deg s^{-2}, respectively. As angular velocity and acceleration derive from the combination of frequency and amplitude of the head oscillations, the decreasing frequency with development led to a decrease of the angular head velocity and acceleration with growth (Fig. 5C,D; regression of total length against median angular velocity: $r^2=0.24$, $P=0.01$; regression of total length against median angular acceleration: $r^2=0.43$, $P=0.0004$). In small larvae, the maximal values for head velocity and acceleration reached ∼2500 deg s^{-1} and ∼250,000 deg s^{-2}, respectively; in contrast, in larger animals, the maximal values were ∼1000 deg s^{-1} for angular velocity and ∼50,000 deg s^{-2} for angular acceleration.

In contrast to the developmental changes in angular head motion parameters, the absolute forward velocity during swimming was comparable between smaller and larger animals (Fig. 5E; regression of total body length against median forward velocity in mm s^{-1}, $P=0.06$). However, when calculating swimming speed with respect to body length, smaller animals swam faster than larger larvae (Fig. 5F; regression of total body length against median forward velocity in body lengths per second, $r^2=0.28$, $P=0.006$). Based on the forward velocity and the size of each animal, *Re* was calculated (as total length multiplied by forward velocity in mm s^{-1} divided by the kinematic viscosity of water at 17°C; see Materials and methods). The *Re* values ranged from ∼150 for slow-swimming small larvae to ∼1500 for fast-swimming large tadpoles with a gradual size-related increase (data not shown; regression of total body length against median *Re*: $r^2=0.64$, $P<0.0001$). Only 4 out of 25 animals had a median *Re*<200, which is considered by some authors to be the boundary between intermediate and inertial hydrodynamic regimes (Fuiman and Webb, 1988; but see also McHenry and Lauder, 2005).

Comparing free and fictive swimming

To determine the relationship between intrinsically generated locomotor commands in the absence of sensory feedback and actual tail oscillations during free swimming, a set of *in vitro*

Journal of Experimental Biology (2017) 220, 227-236 doi:10.1242/jeb.146449

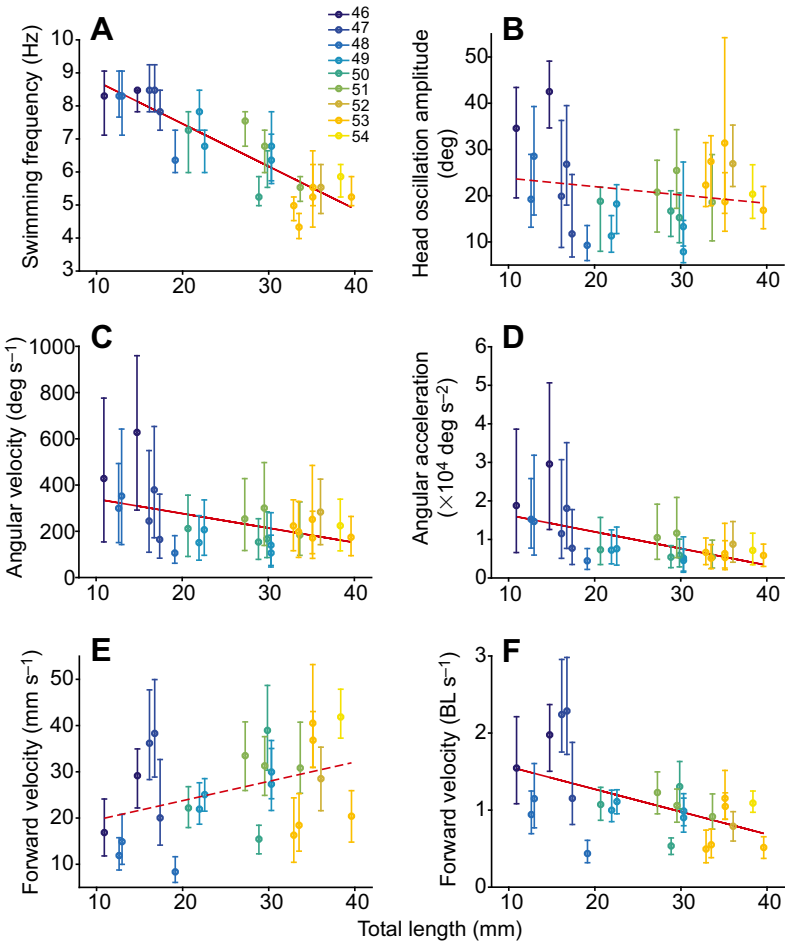

Fig. 5. Changes in kinematic parameters over development. (A–F) Relationship between total body length of the animal and swimming frequency (A), head oscillation amplitude (B), angular velocity (C), angular acceleration (D) and forward velocity in mm s^{-1} (E) and body lengths (BL) s^{-1} (F). All plots show the median and interquartile range obtained for each of N=25 animals; each animal is colour coded according to its developmental stage (key shown in A). The regression of total body length against these kinematic parameters was significant in A (r^2=0.77, P<0.0001), C (r^2=0.24, P=0.01), D (r^2=0.43, P=0.0004) and F (r^2=0.28, P=0.006), but not in B and E, indicating that swimming frequency, angular velocity and acceleration decrease with development, head oscillation amplitude and absolute forward velocity remain unchanged, while the forward velocity in BL s^{-1} decreases. Note the relatively small intra-individual variability of swimming frequency (A).

experiments on semi-intact preparations (Fig. 6A) was conducted. In these experiments, we recorded episodes of fictive swimming, consisting of locomotor activity in the absence of muscle contractions and sensory inputs (see Combes et al., 2004). The bilaterally alternating bursts in ventral roots on both sides recorded in isolated preparations would cause left–right alternating contractions of the axial muscles in the intact animal. Such sequences of fictive swimming, extracellularly recorded as rhythmic burst discharge of ventral roots at the level of spinal segments 8–15, are shown in Fig. 6B. To evaluate temporal changes in the burst rhythm during larval growth, we recorded ventral root spike activity in tadpoles of different sizes (15–45 mm, developmental stages 47–54, N=17). Examples of ventral root recordings in three animals with body lengths of 18, 30 and 42 mm corresponding to developmental stages 47, 50 and 53, respectively, are shown in Fig. 6B. These typical examples revealed a gradual decrease in the burst rhythm frequency with increasing body size. The burst rhythm of larger animals had a lower frequency (see traces on the right of Fig. 6B). In addition, it appeared that individual bursts in smaller animals consisted of fewer spikes compared with those in larger tadpoles, probably due to the presence of more active motoneurons in the larger animals (right trace in Fig. 6B). For quantification, the median burst frequency was determined for each animal (blue circles in Fig. 6C; red encircled dots represent data from the larvae depicted in Fig. 6B) and was plotted along with the frequency of free swimming (black circles in Fig. 6C, data were obtained from Fig. 5A) against body length. In general, the frequency of fictive and free swimming was relatively similar for animals of a given size. In addition, the frequency decreased markedly with body growth both for fictive swimming (Fig. 6C, blue; regression of body length against median fictive swimming frequency: r^2=0.46, P=0.003) and for tail oscillations during free swimming (Fig. 6C, black; slope of best fit for body length against median frequency was −0.13 for free swimming and −0.1 for fictive swimming). However, the intercept exhibited a lower value for fictive swimming (10.03 for free swimming and 8.7 for fictive swimming, Fig. 6C; also compare dashed and solid lines in Fig. 6D; see Discussion).

DISCUSSION

Swimming in *X. laevis* tadpoles is produced by horizontal undulatory tail movements. The tight anatomical connection between the head/body and the tail in these animals causes a strict coupling between axial muscle-driven tail undulations and head oscillations. During the post-embryonic, larval development, when animal length increases ∼3-fold, the swimming frequency concurrently decreases ∼2-fold. As a consequence, both angular velocity and acceleration decrease considerably with larval development, thereby diminishing the dynamic range of angular head motion-related vestibular signals. These results will be compared with those of previous studies on swimming kinematics and developmental changes in *Xenopus* and other species.

Swimming kinematics

Swimming in *Xenopus* tadpoles occurs in two major forms with respect to generated forward velocity and motion consequences for the vestibular organs. Low-speed swimming or cruising is generated by undulations of the most caudal part of the tail, which causes only

Journal of Experimental Biology (2017) 220, 227-236 doi:10.1242/jeb.146449

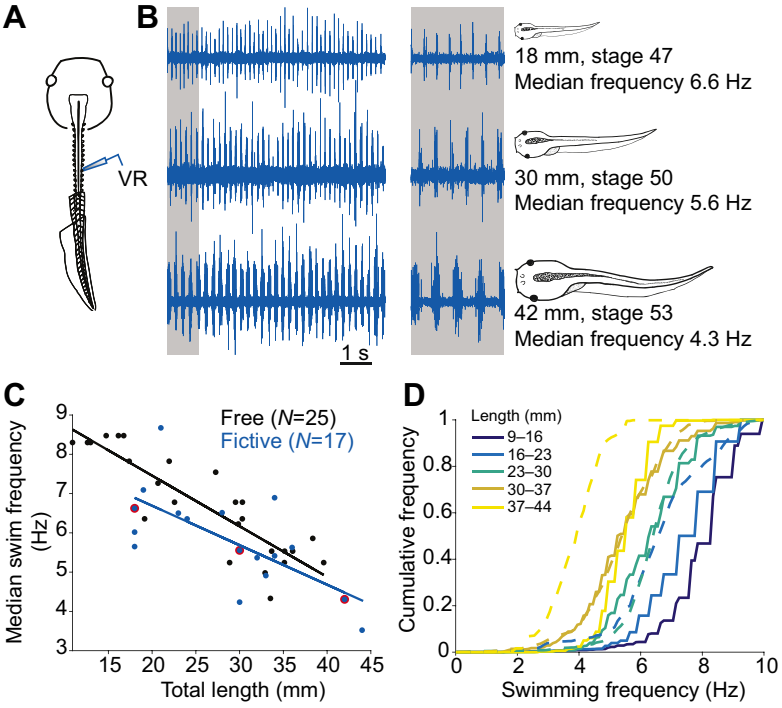

Fig. 6. Comparison of frequencies in free and fictive swimming. (A) Schematic diagram of an isolated, stationary *in vitro* preparation of a tadpole with a suction electrode for recording from a ventral root (VR). (B) Examples of fictive swimming episodes, indicated by rhythmic ventral root discharge, in three differently sized animals: 18 mm (stage 47, top), 30 mm (stage 50, middle) and 42 mm (stage 53, bottom). The first 1 s of swimming is plotted on an extended time scale on the right (grey box), and the median swimming frequency over all episodes of the respective animal is indicated. Tadpole schemes are shown on the same spatial scale (from Hänzi and Straka, 2016a). (C) Relationship between the median frequency of free and fictive swimming and total body length of the animal (the free-swimming data derived from Fig. 5A). Lines show best linear fits, with very similar slopes for free (–0.13, r^2=0.77) and fictive (–0.1, r^2=0.46) swimming. The data for the three animals shown in B are encircled in red. (D) Empirical cumulative distribution of swimming frequency for freely (solid lines; for details on the calculation of instantaneous frequency from the discrete frames, see Material and methods) and fictively swimming preparations (dashed lines). Animals were pooled into five groups according to their body length. Note that the darker traces (indicating smaller animals) are more to the right, in the higher frequency range.

minimal forward thrust and virtually no cyclic left–right head undulations (Hoff and Wassersug, 1986); this mode has also been called 'sculling' and probably serves to hold the vertical position in the water column, as these tadpoles are positively buoyant. In contrast, high-speed swimming is produced by undulations of the entire tail and generates considerable forward velocity as well as cyclic head oscillations, which form angular acceleration stimuli for activating the horizontal semicircular canals. This fast swimming mode, with considerable consequences for vestibular sensation, was examined in the current study. At first glance, this locomotor style seems relatively inefficient, because it appears non-streamlined, but it is exactly this lateral undulatory motion that generates forward thrust (Liu et al., 1997). In the absence of a flexible neck in most fish and tadpole-like amphibian larvae, propulsive swimming-related tail and head movements are tightly coupled and thus allow swimming kinematics to be inferred from head movements (Chagnaud et al., 2012). Moreover, our combined analysis of swimming kinematics and concurrent head motion provided the necessary quantitative information to interpret developmental changes with regard to locomotor dynamics and motion detection capabilities by the vestibular system.

Forward speed is one of the main parameters when describing locomotor behaviour and dynamics. The tadpoles in the current study mostly swam with an absolute speed of 10–60 mm s^{-1}, largely independent of developmental stage, although larger animals generally tended to be slightly faster (Fig. 5E). This magnitude is comparable to the forward speed observed shortly after hatching (45–61 mm s^{-1}; Kahn et al., 1982) as well as to the speed of 6–9 day old zebrafish larvae (Budick and O'Malley, 2000), suggesting that aquatic fish/tadpole-like animals with similar size and morphological shape have comparable locomotor characteristics. However, because of the considerable growth of the body during larval development in *Xenopus*, the forward speed relative to body length decreases from ~1.5 to ~0.5 body lengths per second (BL s^{-1}). This is in marked contrast to a previous study on *Xenopus* tadpoles, in which a swimming speed of around 6 BL s^{-1} was reported (Hoff and Wassersug, 1986). Unfortunately, the small number of animals in that study (*N*=4) and the absence of a description of either developmental stage or size makes it difficult to compare and interpret the noticeable difference from the results of our study.

Swimming frequency is a locomotor parameter of fish and aquatic amphibian locomotor activity that has been widely analysed and thus allows a comparison within and across species. In our study, swimming frequencies of *Xenopus* larvae ranged from 4 to 10 Hz across tadpoles of 10–45 mm, corresponding to larval stages 46–56, and decreased significantly with development. As younger tadpoles below stage 46 (smaller than 14 mm) swim with even higher frequencies shortly after hatching (10–25 Hz; Kahn et al., 1982), this progressive developmental reduction in frequency between hatching and metamorphic climax appears to be a general feature of larval ontogeny. While larval *Xenopus* swim with little frequency variation at each developmental stage, larval zebrafish can express either slow swimming, with frequencies of 25–40 Hz, or burst-like swimming, with frequencies of 45–75 Hz (Budick and O'Malley, 2000). Accordingly, the swimming of *Xenopus* tadpoles is more comparable to the slow swimming mode of larval zebrafish. Swimming frequency is also the parameter that can most easily be compared between free and fictive swimming. This has been done in larval bullfrogs (Stehouwer and Farel, 1980), newt embryos (Soffe et al., 1983), larval angelfish (Yoshida et al., 1996), zebrafish (Lambert et al., 2012b) and young *Xenopus* tadpoles, and in all these cases, free and fictive swimming were found to be at least qualitatively similar. Our current findings add to these previous reports that the swimming frequency is also quantitatively similar between free and fictive swimming, with a gradual developmental decrease of the swim rhythm.

Developmental changes in locomotor patterns

The progressive alteration of the swimming kinematics as the larvae grew from 10 to 45 mm was substantiated by results of previous studies on even younger tadpoles of *X. laevis*. While mostly attached to a substrate between stages 37 and 38 (Boothby and Roberts,

Journal of Experimental Biology (2017) 220, 227-236 doi:10.1242/jeb.146449

1992; Jamieson and Roberts, 2000), the propensity of *Xenopus* larvae to spontaneously swim freely increases after the onset of active feeding at stage 45 (Nieuwkoop and Faber, 1956), as confirmed by a developmental study on fictively swimming animals (Currie et al., 2016). At this time, the frequency of the tail undulations is generally high (10–25 Hz; Kahn and Roberts, 1982; Kahn et al., 1982) and each swimming bout is characterised by decreasing frequencies over the course of the episode (Kahn et al., 1982; Sillar and Roberts, 1993; Sillar et al., 1991). This contrasts with the observation in the older and thus larger tadpoles studied here, where the swimming frequency remains largely constant throughout a given episode (Fig. 4A,B), suggesting that the central pattern generator in the spinal cord at this developmental stage is capable of maintaining a relatively stable rhythm over time. With further developmental progress, the swimming frequency drops fairly linearly (Fig. 5A) to values of 2–4 Hz just before metamorphic climax (Combes et al., 2004; von Uckermann et al., 2016). A likely explanation is that this low tail undulation frequency towards the end of the larval period may derive from the gradually stronger phase coupling of the axial swim rhythm with the concurrently maturating hindlimb kick propulsion that occurs at a lower frequency (Rauscent et al., 2006) and finally replaces the tail-based undulatory swimming as the major locomotor strategy (Combes et al., 2004).

Comparable post-embryonic changes in the frequency of locomotor patterns have also been described in other animals. In rats, the limb movement frequency – tested in water to avoid effects of weak limb musculature – increases during the first 2 weeks after birth (Bekoff and Trainer, 1979); in chickens, the wing-beat frequency increases during the 2 weeks post-hatching (Provine, 1981a); in locusts the wing-beat frequency increases after the final moult (Altman, 1975; Kutsch, 1971, 1974); in moths, the frequency increases before the adult stage is reached, even in the absence of an overt behaviour (Kammer and Kinnamon, 1979). In chickens, the increase starts before and continues after the behaviour (flight) becomes effective (Provine, 1981a). In locusts, the situation is most similar to amphibian tadpoles in the sense that the frequency changes occur after the behaviour (flight/swimming) is implemented (Kutsch, 1971). The increase in locomotor frequency reported in all these examples contrasts with the reduction in tadpole swimming frequency in our study. Nonetheless, all alterations are probably adaptations to optimise or at least maintain locomotor efficiency. Accordingly, the decrease in swim frequency with concurrently increasing body length of the tadpoles might be due either to constraints that the aquatic environment imposes on the swimming of fish-like vertebrates or to the growth-related increase in body rigidity that impairs the execution of flexible tail undulations (Sfakiotakis et al., 1999). In fact, compatible with our results, larger individuals of a given fish species express a slower swim rhythm compared with smaller specimens (Bainbridge, 1957), suggesting that the developmental decrease of the swim rhythm in *Xenopus* tadpoles represents a general feature of growing aquatic vertebrates.

The question arises as to what causes these developmental changes in locomotor frequency. For swimming, hydrodynamic requirements might play a crucial role. For instance, for larval and adult anchovy, which have 'grown out' of the viscous hydrodynamic regime, an intermittent beat-and-glide swimming is more efficient than continuous swimming (Weihs, 1980). This example shows a change in locomotion performance that is related to a change in hydrodynamic regime. Similarly, for larval and juvenile zebrafish, the aquatic environment probably represents a rather viscous regime, whereas adult swimming operates in an inertial regime (McHenry and Lauder, 2005). For tadpoles, Liu et al. (1996) determined a Reynolds number of 7200 for ranid tadpoles with a length of 47 mm at a swim speed of 5 BL s^{-1}. At variance with the locomotor performance of the relatively large and fast amphibian larvae in that study, the generally smaller *Xenopus* tadpoles in our study (15–45 mm) swam at a slower speed, corresponding to a Reynolds number of 300–1500, which is more comparable to that reported for the similarly sized older larvae and adult zebrafish (McHenry and Lauder, 2005). These authors also used body length to calculate *Re*, whereas other authors used a diameter measure for ranid tadpoles (Dudley et al., 1991). A direct comparison of Reynolds numbers obtained in different species is therefore difficult and only allows an approximate inference of the respective locomotor regime (Vogel, 1996). Moreover, different authors define the hydrodynamic regimes differently (Liu et al., 1996; McHenry and Lauder, 2005). Nevertheless, we expect that the vast majority of the tadpoles in our study, with the exception of the smallest larvae, experienced a similar physical regime. Assuming that the most pronounced hydrodynamic changes of locomotor performance in *Xenopus* larvae, as in developing zebrafish, occur at animal lengths of 5–15 mm (Fuiman and Webb, 1988), it is unlikely that hydrodynamics as a critical parameter for aquatic locomotion is the sole driving force for the observed changes in swimming kinematics in the larger tadpoles of our study.

The more general question remains of whether these developmental changes in the frequency of centrally generated locomotor patterns are driven by sensory feedback. In tadpoles, removal of online sensory feedback, as during fictive swimming, slightly reduces the frequency (Fig. 6A); however, this effect is very small compared with the overall developmental decrease. Therefore, the decrease in swimming frequency with increasing body size is a long-term adaptation (according to the terminology of Pearson, 2000). This contrasts with the situation in Australian plague locusts, where the fixation of the wings leads to a frequency similar to that before the developmental change started (Altman, 1975). Sensory feedback in the locust case thus plays an important role on a short time scale. However, this differs on a longer time scale, i.e. the 3 weeks over which the frequency changes, indicating that no practice or sensory feedback is required for the long-term changes to occur (Altman, 1975). This is very similar to the situation in chickens, where the increase in wing flapping over the first 2 weeks post-hatching occurs with featherless wings or wings that were immobilised during those 2 weeks (Provine, 1981a,b) and even in the absence of wings with only wing stumps (Provine, 1979). While these interventions do not abolish sensory feedback completely, they at least suggest that practice of the movements with its associated self-generated sensory feedback is not necessary for the developmental change to occur. Because removal of sensory feedback over a longer time scale is very difficult to achieve in tadpoles, any inference on the impact of such signals on the locomotor output rhythm must necessarily be speculative. The spinal oscillator frequency might change intrinsically without any influence of sensory feedback, or the central effect of sensory feedback might change, or the nature of the sensory feedback might change with development. These possibilities are not mutually exclusive as changes are likely to occur at multiple levels. For instance, the nature of the feedback that the tadpole spinal cord receives directly from the trunk changes over the course of development, from only light touch mediated through Rohon–Beard cells (Roberts and Hayes, 1977) to more extensive proprioceptive feedback via the dorsal roots (Hughes, 1957; Nieuwkoop and Faber, 1956).

Journal of Experimental Biology

Journal of Experimental Biology (2017) 220, 227-236 doi:10.1242/jeb.146449

Consequences of swimming-related head oscillations for vestibular motion detection

The undulatory swimming at all larval stages caused oscillatory head movements with a considerable velocity/acceleration component that forms an adequate stimulus for activating responses in hair cells of the horizontal semicircular canals. The peak angular velocities of head movements that occur during tadpole swimming in the current study exceeded those reported for bucking cattle and spinning dolphins, which are in the range 200–600 deg s^{-1} (Kandel and Hullar, 2010). However, animals that have a body size closer to that of *Xenopus* tadpoles also experience very high angular velocities and accelerations during swimming. In fact, the peak angular velocity generated during undulatory swimming in larval or adult zebrafish reaches up to 10,000 deg s^{-1} (Fontaine et al., 2008) and thus is approximately an order of magnitude larger than that observed during swimming in *Xenopus* tadpoles throughout most of the pre-metamorphic period. During routine swimming, larval zebrafish reach an angular velocity of 4000–10,000 deg s^{-1} and up to 32,000 deg s^{-1} during escape responses (Budick and O'Malley, 2000). Most of the difference in the magnitude of swimming-related head dynamics between *Xenopus* and zebrafish is probably due to the substantially higher swimming frequency in the latter species, which reaches up to 70 Hz (see above). As larval *Xenopus* hatchlings also swim with a higher frequency than older and thus larger larvae (Sillar et al., 1991), it is likely that higher angular velocities are regularly reached.

Detection of head movements by the vestibular system depends both on the magnitude of the head movements and on the overall sensitivity of the sensory structures. The sensitivity of semicircular canals depends on sufficiently large lumen and circuit radii to allow the inertial forces to generate an acceleration-induced and endolymph-mediated cupula displacement (Muller, 1999). This is particularly critical in vertebrates, which develop through small-sized larvae such as fish and amphibians. In fact, the horizontal angular vestibulo-ocular reflex (VOR) in *Xenopus* tadpoles has a relatively late ontogenetic onset (stage 48) that depends on the acquisition of a sufficiently large semicircular canal lumen diameter (Lambert et al., 2008), a finding that also applies to zebrafish (Beck et al., 2004). The interpretation of the physiological findings depended on the assumption that natural angular head movements in *Xenopus* tadpoles occur largely within the range of the experimentally employed horizontal accelerations and do not exceed 400 deg s^{-2} (Lambert et al., 2008). However, the much higher angular accelerations during free swimming in the current study would allow the detection of self-generated head movements with even smaller semicircular canals, suggesting an earlier functional onset of the angular VOR in *Xenopus* tadpoles. Accordingly, the detection of swimming-related horizontal head oscillations and VOR-driven gaze stabilisation might therefore occur immediately after semicircular canal formation at stage 46 (Haddon and Lewis, 1991). However, at least in older animals (stage 55), a locomotor efference copy suppresses the signals from the horizontal semicircular canals during swimming (Chagnaud et al., 2015; Lambert et al., 2012a). This mechanism might already be implemented at younger stages, compatible with the necessity of efference copy-mediated adjustments of the sensory sensitivity, including a considerable attenuation of the sensory inputs. Thus, even though young *Xenopus* larvae generate very high angular accelerations during self-motion, these stimuli might be ineffective for activating an angular VOR, thereby maintaining the overall validity of the earlier study on the ontogeny of gaze stabilisation (Lambert et al., 2008).

Conclusions

Our results show that individual *Xenopus* tadpoles swim with a relatively constant frequency, while the amplitude of the head oscillations is rather variable. During development, the average amplitude of the swimming-related head oscillations remains similar, whereas the frequency decreases as tadpoles grow. Accordingly, this causes a decrease of the angular head velocity and acceleration in older larvae. Surprisingly, younger animals swam faster than older animals if the speed was expressed in terms of body length. Finally, the similarity of free and fictive swimming frequency in tadpoles of a given size along with the concurrent developmental decrease of swimming frequency under both experimental conditions suggests a dominant of the central pattern generator in determining the swim rhythm.

Acknowledgements

The authors thank Dr Larry Hoffman for initiating these experiments and for valuable discussions of the data.

Competing interests

The authors declare no competing or financial interests.

Author contributions

Investigation, Software, Visualization: S.H.; Supervision, Project administration, Funding acquisition: H.S.; Conceptualization, Writing: S.H. and H.S.

Funding

This study was funded by the Deutsche Forschungsgemeinschaft (STR 478/3-1) and the Bundesministerium für Bildung und Forschung (grant number 01 GQ 1407).

Data availability

Data are available from figshare at https://figshare.com/s/e9e7d4dc6b78c72f1151.

Supplementary information

Supplementary information available online at
http://jeb.biologists.org/lookup/doi/10.1242/jeb.146449.supplemental

References

Altman, J. S. (1975). Changes in the flight motor pattern during the development of the Australian plague locust, *Chortoicetes terminifera*. *J. Comp. Physiol. A* **97**, 127-142.

Bainbridge, B. Y. R. (1957). The speed of swimming of fish as related to size and the frequency and amplitude of the tail beat. *J. Exp. Biol.* **35**, 109-133.

Beck, J. C., Gilland, E., Tank, D. W. and Baker, R. (2004). Quantifying the ontogeny of optokinetic and vestibuloocular behaviors in zebrafish, medaka, and goldfish. *J. Neurophysiol.* **92**, 3546-3561.

Bekoff, A. and Trainer, W. (1979). The development of interlimb co-ordination during swimming in postnatal rats. *J. Exp. Biol.* **83**, 1-11.

Boothby, K. M. and Roberts, A. (1992). The stopping response of *Xenopus laevis* embryos: behaviour, development and physiology. *J. Comp. Physiol. A.* **170**, 171-180.

Brustein, E., Saint-Amant, L., Buss, R. R., Chong, M., McDearmid, J. R. and Drapeau, P. (2003). Steps during the development of the zebrafish locomotor network. *J. Physiol. Paris* **97**, 77-86.

Budick, S. A. and O'Malley, D. M. (2000). Locomotor repertoire of the larval zebrafish: swimming, turning and prey capture. *J. Exp. Biol.* **203**, 2565-2579.

Carriot, J., Jamali, M., Chacron, M. J. and Cullen, K. E. (2014). Statistics of the vestibular input experienced during natural self-motion: implications for neural processing. *J. Neurosci.* **34**, 8347-8357.

Chagnaud, B. P., Simmers, J. and Straka, H. (2012). Predictability of visual perturbation during locomotion: implications for corrective efference copy signaling. *Biol. Cybern.* **106**, 669-679.

Chagnaud, B. P., Banchi, R., Simmers, J. and Straka, H. (2015). Spinal corollary discharge modulates motion sensing during vertebrate locomotion. *Nat. Commun.* **6**, 7982.

Combes, D., Merrywest, S., Simmers, J. and Sillar, K. (2004). Developmental segregation of spinal networks driving axial and hindlimb-based locomotion in metamorphosing *Xenopus laevis*. *J. Physiol.* **559**, 17-24.

Currie, S. P., Combes, D., Scott, N. W., Simmers, J. and Sillar, K. T. (2016). A behaviourally-related developmental switch in nitrergic modulation of locomotor rhythmogenesis in larval *Xenopus* tadpoles. *J. Neurophysiol.* **115**, 1446-1457.

Dudley, R., King, V. A. and Wassersug, R. J. (1991). The implications of shape and metamorphosis for drag forces on a generalized pond tadpole (*Rana catesbeiana*). *Copeia* **1**, 252-257.
Fontaine, E., Lentink, D., Kranenbarg, S., Müller, U. K., van Leeuwen, J. L., Barr, A. H. and Burdick, J. W. (2008). Automated visual tracking for studying the ontogeny of zebrafish swimming. *J. Exp. Biol.* **211**, 1305-1316.
Fuiman, L. A. and Webb, P. W. (1988). Ontogeny of routine swimming activity and performance in zebra danios (Teleostei: Cyprinidae). *Anim. Behav.* **36**, 250-261.
Haddon, C. and Lewis, J. (1991). Hyaluronan as a propellant for epithelial movement: the development of semicircular canals in the inner ear of *Xenopus*. *Development* **112**, 541-550.
Hänzi, S. and Straka, H. (2016a). *Schemes of Xenopus laevis tadpoles*. figshare https://dx.doi.org/10.6084/m9.figshare.3841173.v1.
Hänzi, S. and Straka, H. (2016b). *Xenopus laevis: overview over late tadpole stages*. figshare https://dx.doi.org/10.6084/m9.figshare.3839991.v1.
Hänzi, S., Banchi, R., Straka, H. and Chagnaud, B. P. (2015). Locomotor corollary activation of trigeminal motoneurons: coupling of discrete motor behaviors. *J. Exp. Biol.* **218**, 1748-1758.
Harland, R. M. and Grainger, R. M. (2011). *Xenopus* research: metamorphosed by genetics and genomics. *Trends Genet.* **27**, 507-515.
Hoff, K. and Wassersug, R. (1986). The kinematics of swimming in larvae of the clawed frog, *Xenopus laevis*. *J. Exp. Biol.* **122**, 1-12.
Hughes, A. (1957). The development of the primary sensory system in *Xenopus laevis* (Daudin). *J. Anat.* **91**, 323-338.
Jamieson, D. and Roberts, A. (2000). Responses of young *Xenopus laevis* tadpoles to light dimming: possible roles for the pineal eye. *J. Exp. Biol.* **203**, 1857-1867.
Kahn, J. A. and Roberts, A. (1982). The central nervous origin of the swimming motor pattern in embryos of *Xenopus laevis*. *J. Exp. Biol.* **99**, 185-196.
Kahn, J. A., Roberts, A. and Kashin, S. M. (1982). The neuromuscular basis of swimming movements in embryos of the amphibian *Xenopus laevis*. *J. Exp. Biol.* **99**, 175-184.
Kammer, A. E. and Kinnamon, S. C. (1979). Maturation of the flight motor pattern without movement in *Manduca sexta*. *J. Comp. Physiol. A* **130**, 29-37.
Kandel, B. M. and Hullar, T. E. (2010). The relationship of head movements to semicircular canal size in cetaceans. *J. Exp. Biol.* **213**, 1175-1181.
Kutsch, W. (1971). The development of the flight pattern in the desert locust, *Schistocerca gregaria*. *Z. Vgl. Physiol.* **74**, 156-168.
Kutsch, W. (1974). The influence of the wing sense organs on the flight motor pattern in maturing adult locusts. *J. Comp. Physiol.* **88**, 413-424.
Lambert, F. M., Beck, J. C., Baker, R. and Straka, H. (2008). Semicircular canal size determines the developmental onset of angular vestibuloocular reflexes in larval *Xenopus*. *J. Neurosci.* **28**, 8086-8095.
Lambert, F. M., Combes, D., Simmers, J. and Straka, H. (2012a). Gaze stabilization by efference copy signaling without sensory feedback during vertebrate locomotion. *Curr. Biol.* **22**, 1649-1658.
Lambert, A. M., Bonkowsky, J. L. and Masino, M. A. (2012b). The conserved dopaminergic diencephalospinal tract mediates vertebrate locomotor development in zebrafish larvae. *J. Neurosci.* **32**, 13488-13500.
Liu, H., Wassersug, R. and Kawachi, K. (1996). A computational fluid dynamics study of tadpole swimming. *J. Exp. Biol.* **199**, 1245-1260.
Liu, H., Wassersug, R. and Kawachi, K. (1997). The three-dimensional hydrodynamics of tadpole locomotion. *J. Exp. Biol.* **200**, 2807-2819.
McHenry, M. J. and Lauder, G. V. (2005). The mechanical scaling of coasting in zebrafish (*Danio rerio*). *J. Exp. Biol.* **208**, 2289-2301.
Muller, M. (1999). Size limitations in semicircular duct systems. *J. Theor. Biol.* **198**, 405-437.
Nieuwkoop, P. D. and Faber, J. (1956). *Normal Table of Xenopus Laevis (Daudin)*. Amsterdam: North-Holland Publishing Company. Guilders.
Pearson, K. G. (2000). Neural adaptation in the generation of rhythmic behavior. *Annu. Rev. Physiol.* **62**, 723-753.
Provine, R. R. (1979). “Wing-flapping” develops in wingless chicks. *Behav. Neural Biol.* **27**, 233-237.
Provine, R. R. (1981a). Development of wing-flapping and flight in normal and flap-deprived domestic chicks. *Dev. Psychobiol.* **14**, 279-291.
Provine, R. R. (1981b). Wing-flapping develops in chickens made flightless by feather mutations. *Dev. Psychobiol.* **14**, 481-486.
Rauscent, A., Le Ray, D., Cabirol-Pol, M.-J., Sillar, K. T., Simmers, J. and Combes, D. (2006). Development and neuromodulation of spinal locomotor networks in the metamorphosing frog. *J. Physiol. Paris* **100**, 317-327.
Roberts, A. and Hayes, B. P. (1977). The anatomy and function of “free” nerve endings in an amphibian skin sensory system. *Proc. R. Soc. B Biol. Sci.* **196**, 415-429.
Roberts, A., Li, W.-C., Soffe, S. R. and Mclean, D. (2010). How neurons generate behavior in a hatchling amphibian tadpole: an outline. *Front. Behav. Neurosci.* **4**, 16.
Saint-Amant, L. and Drapeau, P. (1998). Time course of the development of motor behaviors in the zebrafish embryo. *J. Neurobiol.* **37**, 622-632.
Sfakiotakis, M., Lane, D. M. and Davies, J. B. C. (1999). Review of fish swimming modes for aquatic locomotion. *IEEE J. Ocean. Eng.* **24**, 237-252.
Sillar, K. and Roberts, A. (1993). Control of frequency during swimming in *Xenopus* embryos: a study on interneuronal recruitment in a spinal rhythm generator. *J. Physiol.* **472**, 557-572.
Sillar, K. T., Wedderburn, J. F. S., Simmers, A. J. and Simmers, A. J. (1991). The development of swimming rhythmicity in post-embryonic *Xenopus laevis*. *Proc. R. Soc. B Biol. Sci.* **246**, 147-153.
Soffe, S. R., Clarke, J. D. W. and Roberts, A. (1983). Swimming and other centrally generated motor patterns in newt embryos. *J. Comp. Physiol. A.* **152**, 535-544.
Stehouwer, D. J. and Farel, P. B. (1980). Central and peripheral controls of swimming in anuran larvae. *Brain Res.* **195**, 323-335.
Straka, H. and Simmers, J. (2012). *Xenopus laevis*: an ideal experimental model for studying the developmental dynamics of neural network assembly and sensory-motor computations. *Dev. Neurobiol.* **72**, 649-663.
Straka, H., Zwergal, A. and Cullen, K. E. (2016). Vestibular animal models: contributions to understanding physiology and disease. *J. Neurol.* **263**, 10-23.
Vogel, S. (1996). *Life in Moving Fluids: The Physical Biology of Flow*. Princeton, N.J: Princeton University Press.
von Uckermann, G., Lambert, F. M., Combes, D., Straka, H. and Simmers, J. (2016). Adaptive plasticity of spino-extraocular motor coupling during locomotion in metamorphosing *Xenopus laevis*. *J. Exp. Biol.* **219**, 1110-1121.
Wallingford, J. B., Liu, K. J. and Zheng, Y. (2010). *Xenopus*. *Curr. Biol.* **20**, R263-R264.
Wark, B., Lundstrom, B. N. and Fairhall, A. (2007). Sensory adaptation. *Curr. Opin. Neurobiol.* **17**, 423-429.
Weihs, D. (1980). Energetic significance of changes in swimming modes during growth of larval anchovy, *Engraulis mordax*. *Fish. Bull.* **77**, 597-604.
Yoshida, M., Matsuura, K. and Uematsu, K. (1996). Developmental changes in the swimming behavior and underlying motoneuron activity in the larval angelfish, *Pterophyllum scalare*. *Zoolog. Sci.* **13**, 229-234.

Supplemental video 1. Example swimming episode of a 13 mm, stage 47 tadpole shown at 200 frames per second. The associated kinematic parameters are shown on the left in Fig. 3.

Supplemental video 2. Example swimming episode of a 38 mm, stage 53 tadpole shown at 200 frames per second. The associated kinematic parameters are shown on the right in Fig. 3.